Journal of Magnetic Resonance 203 (2010) 253–256

Contents lists available at ScienceDirect

Journal of Magnetic Resonance

journal homepage: www.elsevier.com/locate/jmr

^{1}H-detected ^{1}H–^{1}H correlation spectroscopy of a stereo-array isotope labeled amino acid under fast magic-angle spinning

Hiroki Takahashi [a], Masatsune Kainosho [b,c], Hideo Akutsu [a], Toshimichi Fujiwara [a,*]

[a] Institute for Protein Research, Osaka University, 3-2 Yamadaoka, Suita, Osaka 565-0871, Japan
[b] Graduate School of Science, Nagoya University, Furo-cho, Chikusa-ku, Nagoya 464-8602, Japan
[c] Center for Priority Areas, Tokyo Metropolitan University, 1-1 Minami-ohsawa, Hachioji, Tokyo 192-0397, Japan

ARTICLE INFO

Article history:
Received 21 November 2009
Available online 15 January 2010

Keywords:
Magic-angle spinning
Isotope labeling
Solid-state ^{1}H NMR
Amino acid
Protein
^{1}H–^{1}H distance measurement

ABSTRACT

The combined use of selective deuteration, stereo-array isotope labeling (SAIL), and fast magic-angle spinning effectively suppresses the ^{1}H–^{1}H dipolar couplings in organic solids. This method provided the high-field ^{1}H NMR linewidths comparable to those achieved by combined rotation and multiple-pulse spectroscopy. This technique was applied to two-dimensional ^{1}H-detected ^{1}H–^{1}H polarization transfer CHH experiments of valine. The signal sensitivity for the ^{1}H-detected CHH experiments was greater than that for the ^{13}C-detected ^{1}H–^{1}H polarization transfer experiments by a factor of 2–4. We obtained the ^{1}H–^{1}H distances in SAIL valine by CHH experiments with an accuracy of about 0.2 Å by using a theory developed for ^{1}H–^{1}H polarization transfer in ^{13}C-labeled organic compounds.

1. Introduction

Measurement of ^{1}H–^{1}H distances is widely used to analyze 3D molecular structures in solution NMR such as nuclear Overhauser effect spectroscopy (NOESY) [1,2]. Many ^{1}H–^{1}H distance correlations are obtained by low γ nuclei, ^{13}C/^{15}N, detection in solid state NMR [3–9]. In these solid-state experiments, a ^{1}H–^{1}H mixing period sandwiched by CH/NH cross-polarization (CP) connects the ^{13}C/^{15}N evolution and detection periods under isotropic chemical shifts. However, the signal sensitivity of low γ nuclei is much lower than that of proton in principle [10]. The CP efficiency depending on the ^{1}H-spin systems complicates the quantitative analysis and reduces the sensitivity of ^{1}H–^{1}H polarization transfer experiments. These problems can be solved by direct ^{1}H detection in ^{1}H–^{1}H transfer experiments.

In solids, however, it is difficult to obtain high-resolution ^{1}H NMR spectra, because the ^{1}H chemical shift differences are often comparable to the linewidths of signals broadened by the strong homonuclear dipolar interactions. The resolution of ^{1}H NMR spectra can be improved by narrowing the linewidth. First, combined rotation and multiple-pulse spectroscopy (CRAMPS) reduces the linewidth to 0.1–1 ppm for rigid solids at the expense of chemical shift scaling [11–17]. Windowless multiple-pulse sequences provide higher resolution under higher spinning frequencies by indirect detection in 2D NMR [15–17]. Second, magic-angle spinning (MAS) with the frequencies faster than about 30 kHz also enables high-resolution ^{1}H NMR experiments by using small rotors especially at high fields [18–22]. However, the limitation in sample amount leads to low sensitivity. Third, the resolution of ^{1}H NMR spectra is improved by ^{1}H-spin dilution [23–29]. The ^{1}H linewidths of 0.2 ppm have been attained by random deuteration of an amino acid with MAS at moderate spinning frequencies [23,27]. However, nonselectivity in random deuteration entails sensitivity reduction due to low ^{1}H abundance. In contrast, selective deuteration has demonstrated the usefulness for proteins where only hydrogens exchangeable with water are fully protonated, although this method can be applied only to water-exchangeable hydrogens. The linewidths of the amide protons were about 0.5 ppm [24].

In this study, we show high-resolution ^{1}H NMR spectra obtained by combined use of the second and third approaches, i.e. fast MAS and ^{1}H dilution. We selectively diluted an amino acid by using novel deuteration technique, stereo-array isotope labeling (SAIL) developed by Kainosho and co-workers [30,31]. The SAIL amino acids have one proton in methylene groups by stereo-specific replacement with a deuteron and one proton in methyl groups by replacement with two deuterons. Isopropyl groups have only one covalently bonding ^{13}C–^{1}H pair as shown in the inset of Fig. 1. Thus, SAIL method attenuates strong dipolar coupling networks of ^{1}H spins and removes overlaps of ^{1}H signals without losing the sensitivity and the information for protein structures. We have utilized SAIL valine under fast MAS. We compare ^{1}H detection

* Corresponding author. Fax: +81 6 6879 8599.
E-mail address: tfjwr@protein.osaka-u.ac.jp (T. Fujiwara).

1090-7807/$ - see front matter © 2010 Elsevier Inc. All rights reserved.
doi:10.1016/j.jmr.2010.01.005

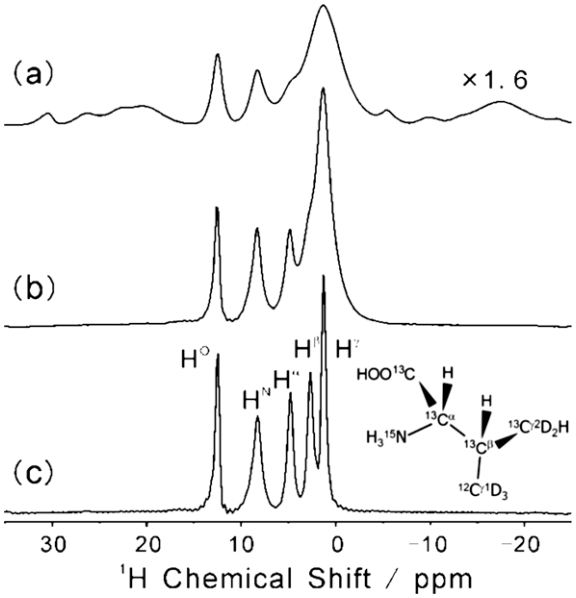

Fig. 1. 1D MAS ^{1}H NMR spectra of uniformly ^{13}C,^{15}N-labeled valine (a,b) and SAIL valine (c) with spinning frequency 12.5 kHz (a) and 27.0 kHz (b,c). Background ^{1}H signals were suppressed by using the ^{13}C-filter pulse sequence in Fig. 2b (see Section 4 for details). SAIL valine structure under an acidic condition is also shown.

and ^{13}C detection of ^{1}H–^{1}H correlations. Finally, we present the distance analysis by the ^{1}H-detected ^{1}H–^{1}H correlation spectroscopy.

2. Results and discussion

2.1. 1D MAS ^{1}H NMR spectra of isotope-labeled valine

Fig. 1 shows 1D ^{13}C-filtered ^{1}H NMR spectra of uniformly ^{13}C,^{15}N-labeled valine and SAIL valine obtained under MAS at a ^{1}H NMR frequency of 700 MHz. Proton resonances at α, β and γ1,2 in valine were not resolved at the spinning frequency of 12.5 kHz for uniformly labeled valine. The increase of the spinning frequency to 27 kHz allowed the distinction of the α proton signal from the large signal consisting of β and γ1,2 resonances. SAIL that eliminates five methyl protons in valine gave well-resolved ^{1}H signals as seen in Fig. 1c. The linewidths of β and γ2 protons decreased by a factor of 2.9 and 3.7, respectively, as shown in Table 1. Thus the elimination of protons as in SAIL valine suppresses strong dipolar couplings. This leads to sensitivity enhancement of all the signals. A single γ2-proton in SAIL valine gave intensity about 1.3 times stronger than that for six protons in uniformly labeled valine for an equal amount of samples.

2.2. 2D ^{1}H/^{13}C-detected ^{1}H–^{1}H polarization transfer experiments

SAIL amino acid along with fast MAS under a high static field permits the measurement of high-resolution ^{1}H–^{1}H correlation with direct ^{1}H detection. Fig. 3 compares a ^{1}H-detected CHH spectrum with a ^{13}C-detected CHHC spectrum for SAIL valine at the MAS frequency of 27 kHz. Pulse sequences for two-dimensional CHHC [3–9] and CHH [32] ^{1}H–^{1}H polarization transfer experiments are shown in Fig. 2. The prepared initial ^{13}C magnetization is modulated by the ^{13}C chemical shifts during the t_1 period. The ^{13}C magnetization is transferred to ^{1}H at the beginning of the ^{1}H–^{1}H dipolar mixing period with CP. After the mixing period, the ^{1}H magnetization is directly detected or transferred back to the ^{13}C for the detection under heteronuclear decoupling fields.

Cross peaks C^{α}/H^{α}, C^{β}/H^{β} and $C^{\gamma 2}/H^{\gamma 2}$ in the CHH spectrum and diagonal peaks in the CHHC spectrum come from the spins that took the same coherence transfer pathways except the third CP and the final detection. Although 1D ^{1}H signals have linewidths larger than ^{13}C signal by more than five times in Hz, the ^{1}H-detected CHH experiment give the α, β and γ peaks larger than the corresponding ^{13}C-detected peaks by a factor of 2.5, 2.1 and 4.4 in S/N, respectively. The CHH experiment gave a larger number of cross peaks than the CHHC experiment partly because of the higher sensitivity of the CHH experiment. The CHHC experiment gave the α/β and β/γ2 cross peaks, while the CHH experiment gave the α/β, β/γ2, $\alpha/\gamma 2$ α/H^N, β/H^N and C^O/H^N peaks. Here, amide and hydroxyl protons do not bond directly to ^{13}C. The methyl peak intensities in the CHHC spectrum were especially smaller than those in the CHH spectrum, because the contact time of the third CP was optimized for the methine proton. Thus, the intensities of the CHHC signals depend largely on the efficiency of the third CP from ^{1}H to ^{13}C. In our previous work on the CHHC sequence [9], we had to perform two experiments different in contact time to obtain the complete correlations: one optimized for CH^{α}–CH^{β} correlation and the other for CH^{α}–$CH^{\gamma}{}_3$. A single ^{1}H-detected CHH experiment, however, yielded the two correlations for CH and CH_3. Therefore, CHH experiments for the SAIL amino acid have not only higher sensitivity but also higher time-efficiency than the CHHC experiment. It was reported that an increase in MAS frequency enhances the sensitivities of ^{1}H-detected CH correlation experiments relative to those of ^{13}C-detected ones at high fields [19]. Since SAIL suppresses the homonuclear couplings similarly to the increase in MAS frequency, SAIL should further enhance the advantage of the ^{1}H detection also in the CH correlation spectroscopy.

Table 1
Linewidths of 1D MAS ^{1}H NMR signals shown in Fig. 1.

Sample	MAS frequency (kHz)	Linewidths[a] (ppm)				
		HO	HN	Hα	Hβ	Hγ2
u-Valine	12.5	0.88	1.1	1.2	2.1	3.5
u-Valine	27	0.61	1.1	0.97	1.8	1.9
SAIL valine	27	0.48	1.1	0.66	0.62	0.52

[a] Linewidths were measured by fitting Lorentzian functions to experimental signals.

2.3. ^{1}H–^{1}H distance measurements for SAIL valine

Finally, we measured ^{1}H–^{1}H distances for H^{α}–H^{β}, H^{α}–$H^{\gamma 2}$, and H^{α}–H^N spin pairs by quantitative analysis of the initial build-up

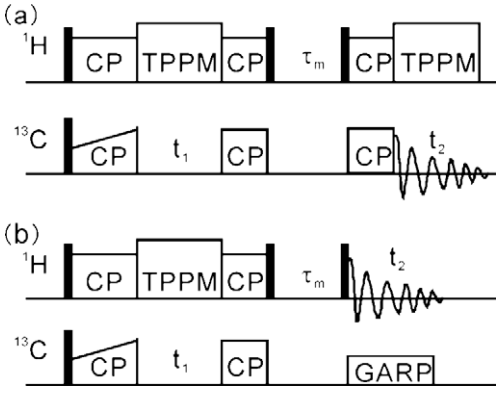

Fig. 2. Pulse sequences for 2D high-resolution ^{13}C-resolved ^{1}H–^{1}H polarization transfer experiments with ^{13}C detection (a) and ^{1}H detection (b). The initial ^{13}C magnetization is prepared mainly by ramped-amplitude CP from the ^{1}H magnetization. The sequences have the ^{13}C chemical shifts evolution period for t_1. After the ^{1}H–^{1}H mixing, the ^{1}H polarization is transferred to ^{13}C in (a) or directly detected in (b).

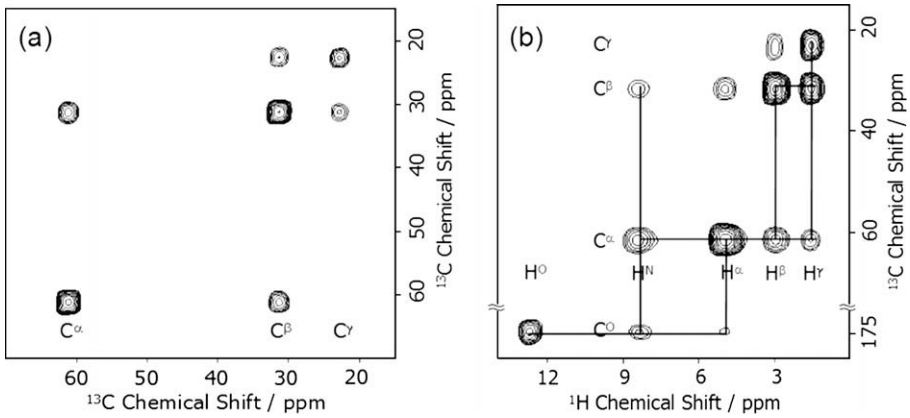

Fig. 3. 2D ^{13}C–^{13}C (a) ^{13}C–^{1}H (b) dipolar correlated NMR spectra of SAIL valine. The ^{1}H–^{1}H mixing time was 593 μs. The contour levels in the carbonyl region are lowered by a factor of 3.3 for (b).

curves using a quantum mechanical approach. The transferred polarization from proton 1 to 2 is described by the following equation [9]:

$$M_{1,2}(t) \approx \sin^2 \varsigma \sin^2 \xi t \tag{1}$$

with

$$\tan \varsigma = \frac{d_{eff}}{\lambda|\delta_{eff}|}, \quad \xi = \frac{1}{2}\sqrt{d_{eff}^2 + (1.2\lambda\delta_{eff})^2}, \quad \text{and}$$

$$\lambda = 0.7\frac{d_{eff}}{|\delta_{eff}|} + 0.67. \tag{2}$$

Here, d_{eff} and τ_{eff} are an effective ^{1}H–^{1}H dipolar coupling strength and an isotropic chemical shift difference, respectively. Polarization is normalized so that the source polarization $M_{1,1}(0) = 1.0$. Fig. 4 represents the initial build-up curves obtained by the experiments and Eq. (1) for the polarization transfer from H^{α} to H^{β}, $H^{\gamma 2}$, and H^{N}. Details of the signal quantification are given in Ref. [9]. The build-up curves fitted to experimental signal intensities gave ^{1}H–^{1}H distances of 2.6 Å for H^{α}–H^{β}, 2.9 Å for H^{α}–$H^{\gamma 2}$, and 2.9 Å for H^{α}–H^{N}. These distances, respectively, agree with 2.5 Å, 3.0 Å and 2.7 Å in the neutron diffraction structure within an accuracy of ±0.2 Å [33]. This agreement verifies the validity of the theoretical analysis at a fast MAS frequency near 30 kHz. The CHH experiments for SAIL valine provide distances with higher signal sensitivities than the CHHC experiments for uniformly ^{13}C-labeled valine by a factor of more than 3. We can obtain a larger number of ^{1}H–^{1}H distances by the CHH experiments than by the CHHC experiments as stated previously. Relayed magnetization transfer was not conspicuous under our experimental condition $\tau_{mix} < 0.15$ ms. Sparse ^{1}H dipolar coupling networks in SAIL amino acids would also contribute to longer distance measurements by suppressing the relayed transfer as for NOE measurements in solution NMR [31].

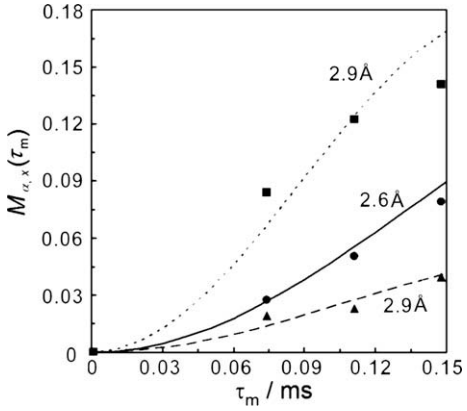

Fig. 4. Experimental polarization amplitudes transferred from $^{1}H^{\alpha}$ to $^{1}H^{\beta}$, $^{1}H^{\gamma 2}$, and $^{1}H^{N}{}_{3}$ are shown as a function of mixing time by circles, triangles, and squares, respectively. The solid, dashed, and dotted lines are calculated by using Eq. (1) with the distances of 2.6, 2.9, and 2.9 Å, respectively. The isotropic chemical shifts of H^{α}, H^{β}, $H^{\gamma 2}$, and H^{N} are 4.8, 2.7, 1.3, and 8.2 ppm, respectively.

3. Conclusions

We have shown high resolution and sensitivity of solid-state ^{1}H NMR of a SAIL amino acid under fast MAS. All the proton signals of SAIL valine were well resolved at the MAS frequency of 27 kHz and the ^{1}H resonance frequency of 700 MHz without using multiple-pulse homonuclear decoupling sequences. The ^{1}H signal intensities in the SAIL amino acid were stronger than those in the uniformly ^{13}C,^{15}N-labeled amino acid owing to attenuation of ^{1}H-homonuclear dipolar couplings. The ^{1}H–^{1}H correlation spectrum of SAIL valine was obtained by the ^{1}H-detected correlation sequence with a sensitivity higher than that by the ^{13}C-detected sequence with a factor of 2–4. Unlike the ^{13}C-detected correlation sequence, the ^{1}H-detected correlation sequence yields the peaks for protons not directly bonding to ^{13}C without the amplitude modulation due to the ^{1}H–^{13}C CP. Thus this ^{1}H-detected ^{1}H–^{1}H correlation spectroscopy of peptides and proteins consisting of SAIL amino acids would be a useful tool for the distance analysis as exemplified for valine.

4. Materials and methods

Pulse sequences for the NMR experiments were shown in Fig. 2. The ^{1}H RF amplitude was 70 kHz for the π/2 pulse, 62 kHz for all CP periods and 85 kHz for the TPPM decoupling sequence consisting of 170° pulses with RF phase shifts of 16° [34]. The ^{13}C RF amplitude was 70 kHz for the π/2 pulse and varied from 30 to 43 kHz in the first CP. The ^{13}C RF field amplitude was switched to 37 kHz for the second and third CP periods. The contact time of the first CP was 2 ms, and that of the second and third CP was 74 μs which was optimized for the polarization transfer by the CH dipolar coupling in methines. The ^{13}C GARP decoupling [35] with amplitude 7 kHz was applied to the ^{1}H detection. Eight FIDs were accumulated with a recycle delay of 5 s. An FID with 512 data points and a dwell time of 20 μs was zero-filled to 1024 points and Fourier-transformed by using Biosym Felix950. The chemical shifts were referenced to 2,2-dimethyl-2-silapentane-5-sulfonate [36]. The 1D ^{1}H NMR spectra in Fig. 1 were obtained with the pulse sequences in Fig. 2b at $\tau_m = 1$ μs and $t_1 = 10$ μs to subtract the

background ^{1}H signals. Experiments were performed at room temperature on a Varian Infinity Plus-700 spectrometer with a broadband triple resonance probe for a 2.5-mmϕ rotor. Uniformly ^{13}C,^{15}N-labeled L-valine hydrochloride (Shoko Co. Ltd., Tokyo, Japan) and SAIL valine hydrochloride were crystallized from a dilute HCl solution [33].

Acknowledgments

This work was partly supported by Grants-in-Aid for Scientific Research KAKENHI, Targeted Protein Programs from MEXT and SENTAN from JST.

References

[1] J. Cavanagh, W. J. Fairbrother, A.G. Palmer III, M. Rance, N. J. Skelton, Protein NMR spectroscopy, second ed., Academic Press, 2007.
[2] P.D. Thomas, V.J. Basus, T.L. James, Protein solution structure determination using distances from two-dimensional nuclear Overhauser effect experiments: effect of approximations on the accuracy of derived structures, Proc. Natl. Acad. Sci. USA 88 (1991) 1237–1241.
[3] S. Zhang, B.H. Meier, R.R. Ernst, Local monitoring of proton spin diffusion in static and rotating samples via spy detection, Solid State Nucl. Magn. Reson. 1 (1993) 313–320.
[4] M. Wilhelm, H. Feng, U. Tracht, H.W. Spiess, 2D CP/MAS ^{13}C isotropic chemical shift correlation established by ^{1}H spin diffusion, J. Magn. Reson. 134 (1998) 255–260.
[5] I. de Boer, L. Bosman, J. Raap, H. Oschkinat, H.J.M. de Groot, 2D ^{13}C–^{13}C MAS NMR correlation spectroscopy with mixing by true 1H spin diffusion reveals long-range intermolecular distance restraints in ultra high magnetic field, J. Magn. Reson. 157 (2002) 286–291.
[6] R. Tycko, Y. Ishii, Constraints on supramolcular structure in amyloid fibrils from two-dimensional solid-state NMR spectroscopy with uniform isotopic labeling, J. Am. Chem. Soc. 125 (2003) 6606–6607.
[7] A. Lange, K. Seidel, L. Verdier, S. Luca, M. Baldus, Analysis of proton–proton transfer dynamics in rotating solids and their use for 3D structure determination, J. Am. Chem. Soc. 125 (2003) 12640–12648.
[8] K. Iwata, T. Fujiwara, Y. Matsuki, H. Akutsu, S. Takahashi, H. Naiki, Y. Goto, 3D structure of amyloid protofilaments of β_2-microglobulin fragment probed by solid-state NMR, Proc. Natl. Acad. Sci. USA 103 (2006) 18119–18124.
[9] H. Takahashi, H. Akutsu, T. Fujiwara, A magic-angle-spinning NMR method for ^{1}H–^{1}H distance measurement using coherent polarization transfer in ^{13}C-labeled organic solids, J. Chem. Phys. 129 (2008) 154504.
[10] M.F. Summers, L.G. Marzilli, Ad. Bax, Complete ^{1}H and ^{13}C assignments of coenzyme B12 through the use of new two-dimensional NMR experiments, J. Am. Chem. Soc. 108 (1986) 4285–4294.
[11] B.C. Gerstein, R.G. Pembleton, R.C. Wilson, L.M. Ryan, High resolution NMR in randomly oriented solids with homonuclear dipolar broadening: combined multiple pulse NMR and magic angle spinning, J. Chem. Phys. 66 (1977) 361–362.
[12] S.F. Dec, C.E. Bronnimann, R.A. Wind, G.E. Maciel, Comparison of the ^{1}H NMR analysis of solids by the CRAMPS and MAS-only techniques, J. Magn. Reson. 82 (1989) 454–466.
[13] B.C. Gerstein, The Encyclopedia of NMR, John Wiley and Sons, London, 1997, pp. 1501–1509.
[14] C. Filip, S. Hafner, Analysis of multiple-pulse techniques under fast MAS conditions, J. Magn. Reson. 147 (2000) 250–260.
[15] D. Sakellarioua, A. Lesagea, P. Hodgkinsonb, L. Emsley, Homonuclear dipolar decoupling in solid-state NMR using continuous phase modulation, Chem. Phys. Lett. 319 (2000) 253–260.
[16] E. Vinogradov, P.K. Madhu, S. Vega, Proton spectroscopy in solid state nuclear magnetic resonance with windowed phase modulated Lee–Goldburg decoupling sequences, Chem. Phys. Lett. 354 (2002) 193–202.
[17] A. Lesage, D. Sakellariou, S. Hediger, B. Eléna, P. Charmonta, S. Steuernagelc, L. Emsley, Experimental aspects of proton NMR spectroscopy in solids using phase-modulated homonuclear dipolar decoupling, J. Magn. Reson. 163 (2003) 105–113.
[18] Y. Ishii, R. Tycko, Sensitivity enhancement in solid state ^{15}N NMR by indirect detection with high-speed magic angle spinning, J. Magn. Reson. 142 (2000) 199–204.
[19] Y. Ishii, J.P. Yesinowski, R. Tycko, Sensitivity enhancement in solid-state ^{13}C NMR of synthetic polymers and biopolymers by ^{1}H NMR detection with high-speed magic angle spinning, J. Am. Chem. Soc. 123 (2001) 2921–2922.
[20] I. Schnell, H.W. Spiess, High-resolution ^{1}H NMR spectroscopy in the solid state: very fast sample rotation and multiple-quantum coherences, J. Magn. Reson. 151 (2001) 153–227.
[21] A. Samoson, T. Tuherm, Z. Gan, High-field high-speed MAS resolution enhancement in ^{1}H NMR spectroscopy of solids, Solid State Nucl. Magn. Reson. 20 (2001) 130–136.
[22] D.H. Zhou, G. Shah, M. Cormos, C. Mullen, D. Sandoz, C.M. Rienstra, Proton-detected solid-state NMR spectroscopy of fully protonated proteins at 40 kHz magic-angle spinning, J. Am. Chem. Soc. 129 (2007) 11791–11801.
[23] A.E. McDermott, F.J. Creuzet, A.C. Kolbert, R.G. Griffin, High-resolution magic-angle-spinning NMR spectra of protons in deuterated solids, J. Magn. Reson. 98 (1992) 408–413.
[24] B. Reif, C.P. Jaroniec, C.M. Rienstra, M. Hohwy, R.G. Griffin, ^{1}H–^{1}H MAS correlation spectroscopy and distance measurements in a deuterated peptide, J. Magn. Reson. 151 (2001) 320–327.
[25] V. Chevelkov, B.J. van Rossum, F. Castellani, K. Rehbein, A. Diehl, M. Hohwy, S. Steuernagel, F. Engelke, H. Oschkinat, B. Reif, ^{1}H detection in MAS solid-state NMR spectroscopy of biomacromolecules employing pulsed field gradients for residual solvent suppression, J. Am. Chem. Soc. 125 (2003) 7788–7789.
[26] E.K. Paulson, C.R. Morcombe, V. Gaponenko, B. Dancheck, R.A. Byrd, K.W. Zilm, Sensitive high resolution inverse detection NMR spectroscopy of proteins in the solid state, J. Am. Chem. Soc. 125 (2003) 15831–15836.
[27] D.H. Zhou, D.T. Graesser, W.T. Franks, C.M. Rienstra, Sensitivity and resolution in proton solid-state NMR at intermediate deuteration levels: quantitative linewidth characterization and applications to correlation spectroscopy, J. Magn. Reson. 178 (2006) 297–307.
[28] V. Chevelkov, K. Rehbein, A. Diehl, B. Reif, Ultrahigh resolution in proton solid-state NMR spectroscopy at high levels of deuteration, Angew. Chem. Int. Ed. 45 (2006) 3878–3881.
[29] V. Agarwal, A. Diehl, N. Skrynnikov, B. Reif, High resolution ^{1}H detected ^{1}H, ^{13}C correlation spectra in MAS solid-state NMR using deuterated proteins with selective ^{1}H,^{2}H isotopic labeling of methyl groups, J. Am. Chem. Soc. 128 (2006) 12620–12621.
[30] T. Torizawa, A.M. Ono, T. Terauchi, M. Kainosho, NMR assignment methods for the aromatic ring resonances of phenylalanine and tyrosine residues in proteins, J. Am. Chem. Soc. 127 (2005) 12620–12626.
[31] M. Kainosho, T. Torizawa, Y. Iwashita, T. Terauchi, A.M. Ono, P. Guntert, Optimal isotope labelling for NMR protein structure determinations, Nature 440 (2006) 52–57.
[32] W. Luo, M. Hong, A 1D sensitivity-enhanced ^{1}H spin diffusion experiment for determining membrane protein topology, Solid State Nucl. Magn. Reson. 29 (2006) 163–169.
[33] T.F. Koetzle, L. Golic, M.S. Lehmann, J.J. Verbist, W.C. Hamilton, Precision neutron diffraction structure determination of protein and nucleic acid components. XV. Crystal and molecular structure of the amino acid L-valine hydrochloride, J. Chem. Phys. 60 (1974) 4690–4696.
[34] A.E. Bennett, C.M. Rienstra, M. Auger, K.V. Lakshmi, R.G. Griffin, Heteronuclear decoupling in rotating solids, J. Chem. Phys. 103 (1995) 6951–6958.
[35] A.J. Shaka, P.B. Barker, R. Freeman, Computer-optimized decoupling scheme for wideband applications and low-level operation, J. Magn. Reson. 64 (1985) 547–552.
[36] C.R. Morcombe, K.W. Zilm, Chemical shift referencing in MAS solid state NMR, J. Magn. Reson. 162 (2003) 479–486.